Induction of Endoplasmic Reticulum Stress *via* Reactive Oxygen Species Mediated by Luteolin in Melanoma Cells

JOON KI KIM[1], KYOUNG AH KANG[2], YEA SEONG RYU[2], MEI JING PIAO[2], XIA HAN[2], MIN CHANG OH[2], SUN JIN BOO[3], SEUNG UK JEONG[3], YONG JOO JEONG[1], SUNGWOOK CHAE[4], SOO-YOUNG NA[3] and JIN WON HYUN[2]

[1]*Department of Bio and Nanochemistry, Kookmin University, Seoul, Republic of Korea;*
[2]*School of Medicine, Jeju National University, Jeju, Republic of Korea;*
[3]*School of Medicine, Jeju National University, Jeju, Republic of Korea;*
[4]*KM Based Herbal Drug Development Group, Korea Institute of Oriental Medicine, Daejeon, Republic of Korea*

Abstract. *Background: This study aimed to investigate whether luteolin, a flavonoid, induces apoptosis in human melanoma cells via endoplasmic reticulum (ER) stress. Materials and Methods: To investigate the effects of luteolin in human melanoma cells, the anti-proliferation, apoptosis, ER stress induction and reactive oxygen species (ROS) generation were evaluated using MTT, Hoechst 33342, ER-tracker Blue White DPX and DCF-DA staining assays, respectively. Results: Luteolin inhibited cell proliferation and increased apoptotic body formation. Luteolin induced ER stress, as shown by ER staining and mitochondrial Ca^{2+} overloading. Luteolin increased expression of the ER stress-related proteins; protein kinase RNA-like ER kinase, phospho eukaryotic translation initiation factor 2α, activating transcription factor (ATF) 6, CCAAT/enhancer-binding protein-homologous protein (CHOP), and cleaved caspase 12. Furthermore, luteolin increased the level of intracellular ROS, leading to ROS-mediated apoptosis and ER stress. However, N-acetyl cysteine, a ROS scavenger, decreased ROS levels, apoptosis, and ER stress induced by luteolin treatment. In addition, knockdown of CHOP and ATF6 by small-interfering RNA inhibited luteolin-induced cell death. Conclusion: Luteolin induces apoptosis by ER stress via increasing ROS levels.*

Melanoma, a malignancy of melanocytes, tends to metastasize to multiple organs *via* the brain, lungs, liver, and bones. Cancer cell types differ in their susceptibility to chemotherapy, and malignant melanoma, one of the most difficult cancers to treat, is largely unresponsive to conventional chemotherapy, resulting in low 5-year survival rates (1, 2). Therefore, it is necessary to find effective compounds against melanoma.

The endoplasmic reticulum (ER) is a specialized organelle that plays fundamental roles in the biology of the cell. ER critically participates in the regulation of intracellular Ca^{2+} levels and synthesis of secretory proteins bound for the cell surface (3). When misfolded proteins accumulate in the ER or Ca^{2+} stores are depleted, ER stress is induced and an evolutionally-conserved unfolded protein response occurs in the cell to maintain homeostasis (4). In higher eukaryotes, ER stress response is mediated by at least three main stress sensors that are all located at the ER, namely, inositol-requiring enzyme 1α, protein kinase RNA-like ER kinase (PERK), and activating transcription factor (ATF) 6 (5). Activation of PERK leads to direct phosphorylation of the ubiquitous eukaryotic translation initiation factor-2α (eIF2α), to rapidly attenuate translation and reduce protein overload in the ER lumen. This mechanism also induces the translation of ATF4, a transcription factor that controls the expression of genes involved in apoptosis, autophagy, amino acid metabolism, and anti-oxidant responses (6). The pro-apoptotic transcription factor CCAAT/enhancer-binding protein-homologous protein (CHOP) inhibits the transcription of Bcl-2. It can be induced by a combination of PERK/ATF4 and ATF6 pathways (7-9). Upon activation of CHOP, cell death occurs *via* apoptosis (10, 11). The mitochondrial apoptotic pathway functions particularly in reactive oxygen species (ROS)-mediated apoptosis. ER stress is induced by accumulation of ROS, leading to mitochondrial dysfunction and apoptosis (12). ROS are mainly generated inside mitochondria; however, mitochondria also have an attractive function in response to oxidative stress (13).

Correspondence to: Jin Won Hyun, School of Medicine, Jeju National University, Jeju 63243, Republic of Korea. E-mail: jinwonh@jejunu.ac.kr and Soo-Young Na, School of Medicine, Jeju National University, Jeju 63241, Republic of Korea. E-mail: sktndud@hanmail.net

Key Words: Luteolin, ER stress, Reactive oxygen species, Ca^{2+} overloading, melanoma.

Recent studies showed that the ER has properties that are somewhat sensitive to oxidative damage and may be considered to have a significant role in the response to oxidative stress-induced damage (12, 14).

Flavonoids are well-known for their wide spectrum of pharmacological properties including anti-oxidant, anti-microbial, and cancer-preventive effects. Among them, luteolin (3',4',5,7-tetrahydroxyflavone) exhibits anti-oxidant, anti-inflammatory, and anticancer activities (15-17). In terms of its anticancer activities, luteolin induces apoptosis *via* extrinsic and/or intrinsic signaling pathways in cancer cells including neuroblastoma cells, breast cancer cells, colon cancer cells, liver cancer cells, and lung cancer cells (18-22). However, little is known on the involvement of ER stress in this process. To address this issue, we investigated whether luteolin-induced apoptosis of human melanoma cells is mediated *via* ER stress.

Materials and Methods

Reagents. Rhod-2 AM and the ER tracker Blue-White DPX dye were purchased from Molecular Probes (Eugene, OR, USA). Hoechst 33342 and luteolin were purchased from Sigma Aldrich (St. Louis, MO, USA). Primary antibodies against phospho PERK, phospho eIF2α, ATF6, and actin were purchased from Santa Cruz Biotechnology (Santa Cruz, CA, USA). Primary antibodies against CHOP and caspase 12 were purchased from Cell Signaling Technology (Beverly, MA, USA).

Cell culture. The human melanoma cell line A2058 was provided by Professor Hoi Young Lee (Konyang University, Nonsan, Republic of Korea). These cells were maintained at 37˚C in an incubator with a humidified atmosphere of 5% CO_2 and cultured in DMEM containing 10% heat-inactivated fetal calf serum, streptomycin (100 μg/ml), and penicillin (100 U/ml).

Cell viability assay. The effect of luteolin on cell viability was determined using the 3-(4,5-dimethylthiazol-2-yl)-2,5-diphenyltetrazolium bromide (MTT) assay, which is based on the reduction of a tetrazolium salt by mitochondrial succinate dehydrogenase in viable cells (23). A2058 cells were seeded into a 96-well plate at a density of 6×10^4 cells/ml, treated with 0-80 μg/ml luteolin, and incubated for 48 h. Next, MTT stock solution (50 μl, 2 mg/ml) were added to each well to attain a total reaction volume of 250 μl. After incubation for 4 h, the supernatants were aspirated. The formazan crystals in each well were dissolved in 150 μl dimethyl sulfoxide, and absorbance at 540 nm was read on a scanning multi-well spectrophotometer.

Colony-forming assay. A2058 cells were seeded at a density of 600 cells per 60-mm dish and cultured for 14 days with 35 μg/ml luteolin. During colony growth, the culture medium was replaced every 3 days. Colonies containing more than 50 cells were included in the assay. The colonies were counted *via* microscopic observation using a Diff-Quick staining kit (Sysmex, Kobe, Japan).

Nuclear staining with Hoechst 33342. A2058 cells were seeded into chamber slides at a density of 6×10^4 cells/ml. At 16 h after plating, the cells were treated with luteolin at a concentration of 35 μg/ml and incubated for 48 h. Hoechst 33342 (3 μl, 10 mg/ml), a DNA-specific fluorescent dye, was added to each well, and cells were incubated for 10 min at 37˚C. Stained cells were visualized under a fluorescence microscope equipped with a CoolSNAP-Pro color digital camera.

ER staining. A2058 cells were seeded at a density of 6×10^4 cells/ml in 6-well plates. At 16 h after plating, the cells were treated with luteolin at a concentration of 35 μg/ml and incubated for 48 h. Cells were harvested, washed, and re-suspended in phosphate-buffered saline (PBS) containing the ER tracker Blue-White DPX dye. After incubation for 30 min at 37˚C, cells were washed, suspended in PBS, and analyzed by flow cytometry. For confocal microscopy imaging analysis, cells were seeded into chamber slides at a density of 6×10^4 cells/ml. At 16 h after plating, cells were treated with luteolin at a concentration of 35 μg/ml and incubated for 48 h. Next, the ER tracker was added to the cells, and the samples were incubated for 30 min at 37˚C. The tracker solution was removed, and the cells were washed with PBS. Microscopy images were collected using LSM 5 PASCAL software.

Measurement of mitochondrial Ca^{2+} levels. Rhod-2 AM was used to determine the levels of mitochondrial Ca^{2+}. Rhod-2 AM has a net positive charge under physiological conditions, which facilitates its sequestration into mitochondria *via* membrane potential-driven uptake. The use of Rhod-2 AM improves the selectivity of mitochondrial loading because the dye exhibits Ca^{2+}-dependent fluorescence only after oxidation, a process that preferentially occurs within mitochondria. A2058 cells were seeded at a density of 6×10^4 cells/ml. At 16 h after plating, cells were treated with luteolin at a concentration of 35 μg/ml and incubated for an additional 48 h. Cells were harvested, washed, and re-suspended in PBS containing the Rhod-2 AM. After incubation for 30 min at 37˚C, cells were washed, suspended in PBS, and analyzed by flow cytometry. For image analysis, cells were loaded with Rhod-2 AM and incubated for 30 min at 37˚C. The stained cells were then washed and mounted onto microscope slides in mounting medium. Microscopy images were obtained using a confocal laser scanning microscope and LSM 5 PASCAL software.

Measurement of intracellular ROS. The dichlorofluorescein diacetate (DCF-DA) method was used to measure levels of intracellular ROS (24). A2058 cells were seeded into 96-well plates at a density of 6×10^4 cells/ml. At 16 h after plating, the cells were treated with luteolin at a concentration of 35 μg/ml. The cells were then incubated for an additional 30 min at 37˚C. Next, DCF-DA solution (25 μM) was added to the cells and incubated for 10 min. The fluorescence of the 2',7'-dichlorofluorescein product was determined using a FACS Calibur flow cytometer (Becton Dickinson, Mountain View, CA, USA).

Western blot analysis. A2058 cells were harvested, washed twice with PBS, lysed on ice for 30 min in 100 μl of lysis buffer containing 120 mM NaCl, 40 mM Tris (pH 8), and 0.1% NP-40, and centrifuged at 13,000 rpm for 5 min. Supernatants were collected from the lysates, and the protein concentrations in the lysates were determined. Aliquots of the lysates (10 μg of protein) were boiled for 5 min and electrophoresed in 10% sodium dodecyl sulfate-polyacrylamide gels. The resolved proteins were then

transferred onto nitrocellulose membranes, which were subsequently incubated with the primary antibodies described above, followed by a horseradish peroxidase-conjugated secondary antibody (Pierce, Rockford, IL, USA). Protein bands were detected using an enhanced chemiluminescence Western blotting detection kit (Amersham, Little Chalfont, Buckinghamshire, UK), followed by exposure of the membranes to X-ray film.

Transient transfection of small-interfering RNA (siRNA). Cells were seeded in 96-well plates at a density of 6×10^4 cells/ml and allowed to reach approximately 50% confluency on the day of transfection. The siRNA constructs used were mismatched control siRNA (siControl RNA), CHOP-targeting siRNA (siCHOP RNA), and ATF6-targeting siRNA (siATF6 RNA) (Santa Cruz Biotechnology). Cells were transfected with 10-50 nM siRNA using Lipofectamine 2000 (Invitrogen, Carlsbad, CA, USA). After 24 h, cells were examined by Western blot analysis and MTT assay.

Statistical analysis. Values are expressed as the mean±standard error of the mean. Data were analyzed using an analysis of variance and Tukey's *post-hoc* test to determine pairwise differences. $p<0.05$ was considered significant.

Results

Inhibition of cell proliferation and induction of apoptosis by luteolin. The ability of luteolin to inhibit the proliferation of A2058 human melanoma cells was assessed using the MTT assay. Luteolin exerted substantial cytotoxicity against A2058 cells in a dose-dependent manner, reducing cell viability to 50% (IC_{50} value) at a concentration of 35 μg/ml (Figure 1A). Based on this result, 35 μg/ml were chosen as the optimal dose of luteolin for further study.

The inhibition of cell proliferation by luteolin (35 μg/ml) was also confirmed by a colony-forming assay. The colony-forming ability revealed a smaller percentage of colonies for luteolin-treated cells than for control cells, when the percentage of control colonies was normalized to 100% (Figure 1B). To assess the apoptotic properties of luteolin, nuclear staining was performed using the Hoechst 33342 dye. Microscopic examination demonstrated increased formation of apoptotic bodies in luteolin-treated cells compared to control cells (Figure 1C).

Induction of ER stress and mitochondrial Ca^{2+} overloading in human melanoma cells by luteolin. ER tracker-stained cells were investigated *via* flow cytometry and fluorescence microscopy. Flow cytometry data indicated a higher fluorescence intensity (FI) of the ER tracker, Blue-White DPX dye, in luteolin-treated cells (FI: 437) than in control cells (FI: 86) (Figure 2A). The fluorescence microscopy data were consistent with the flow cytometry data (Figure 2B). Release of calcium from ER stores induces ER stress, leading to an increase in cytosolic and mitochondrial Ca^{2+} levels (25). Rhod-2 AM-stained cells were investigated *via* flow cytometry and fluorescence microscopy. Flow cytometry data indicated a higher FI of the Rhod-2 AM dye in luteolin-treated cells (FI: 298) than in control cells (FI: 96) (Figure 2C). The fluorescence microscopy data were consistent with the flow cytometry data (Figure 2D).

Induction of ER stress through luteolin-induced ROS generation. Luteolin treatment of A2058 cells resulted in enhanced levels of intracellular ROS concomitant with ER stress. However, N-acetyl cysteine (NAC), an antioxidant/ROS scavenger, decreased the ROS content in luteolin-treated cells (Figure 3A). In addition, NAC attenuated apoptosis and ER stress induced by luteolin treatment, as assessed by Hoechst 33342 and Blue-White DPX dye (Figure 3B and C).

Expression of ER stress-related proteins in luteolin-treated A2058 cells. Expression of ER stress-related proteins, including phospho PERK, phospho eIF2α, ATF6, CHOP, and cleaved caspase 12, was higher in luteolin-treated cells than in control cells (Figure 4A). The putative roles of CHOP and ATF6 in luteolin-treated cells were investigated by siRNA-mediated silencing *in vitro*. siControl RNA-transfected cells with luteolin treatment had a significantly lower viability than siControl RNA-transfected cells (Figure 4B and C). Furthermore, luteolin treatment in siCHOP RNA- or siATF6 RNA-transfected cells significantly recovered cell viability of siControl RNA-transfected cells with luteolin treatment, suggesting that luteolin induces ER stress-mediated cell death *via* CHOP or ATF6 (Figure 4B and C).

Discussion

The aim of this study was to investigate whether luteolin can induce apoptosis *via* an ER stress-related pathway in human melanoma cells. Our findings suggest that luteolin can be utilized as part of therapeutic strategies for the effective management of metastatic melanoma by effectively increasing ER stress and mitochondrial Ca^{2+} levels in A2058 cells. The ER and mitochondria are major calcium stores in cells, and calcium is transferred through a calcium channel (26). ER-mitochondria calcium cross-talk plays a key role in cell signaling to regulate metabolism and induce cell death (27). A change in the Ca^{2+} stores of the ER is associated with ER stress-mediated apoptosis (28). It was recently reported that ER stress stimulates the release of Ca^{2+} into the cytosol, followed by uptake of Ca^{2+} into mitochondria, mitochondrial fission, and release of cytochrome *c*, precipitating apoptosis (29). Apoptotic cross-talk between the ER and mitochondria is dependent on calcium signaling from the ER to mitochondria, which is constrained by Bcl-2 and activated by Bax (30). Furthermore, under ER stress conditions, apoptosis is induced *via* several other mechanisms, including cross-talk between ER and mitochondria as well as Ca^{2+} release from

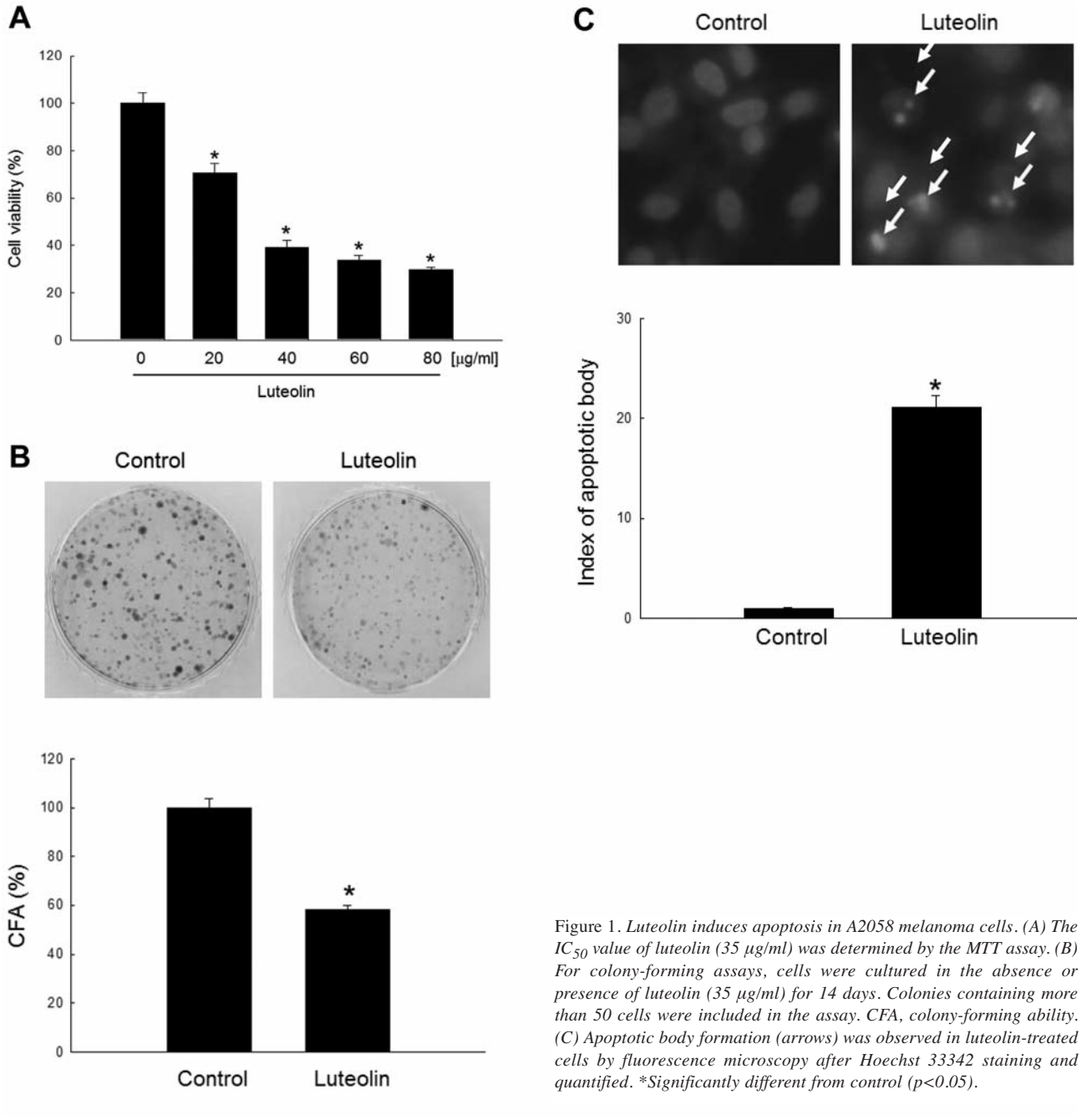

Figure 1. *Luteolin induces apoptosis in A2058 melanoma cells. (A) The IC_{50} value of luteolin (35 μg/ml) was determined by the MTT assay. (B) For colony-forming assays, cells were cultured in the absence or presence of luteolin (35 μg/ml) for 14 days. Colonies containing more than 50 cells were included in the assay. CFA, colony-forming ability. (C) Apoptotic body formation (arrows) was observed in luteolin-treated cells by fluorescence microscopy after Hoechst 33342 staining and quantified. *Significantly different from control ($p<0.05$).*

ER stores through the inositol 1,4,5-triphosphate receptor and ryanodine receptor channels (31). Inositol 1,4,5-triphosphate receptors function as ligand-gated channels that release Ca^{2+} from intracellular Ca^{2+} stores (32). Not only misfolded proteins accumulated in the ER but also Ca^{2+} store depletion leads to ER stress.

Among the various pro-apoptotic regulators, CHOP is a hallmark of programmed cell death that is closely associated with ER stress (33). Luteolin induced the ER stress-related proteins phospho PERK, phospho eIF2α, ATF6, CHOP, and caspase 12. ROS increases apoptosis *via* ER stress and mitochondria dysfunction (34). Luteolin-treated cells had increased intracellular ROS levels; however, pre-treatment with an anti-oxidant attenuated luteolin-induced apoptosis and ER stress in A2058 cells. These findings suggest that luteolin treatment triggers apoptosis in human melanoma cells through a mechanism involving ROS-mediated ER stress.

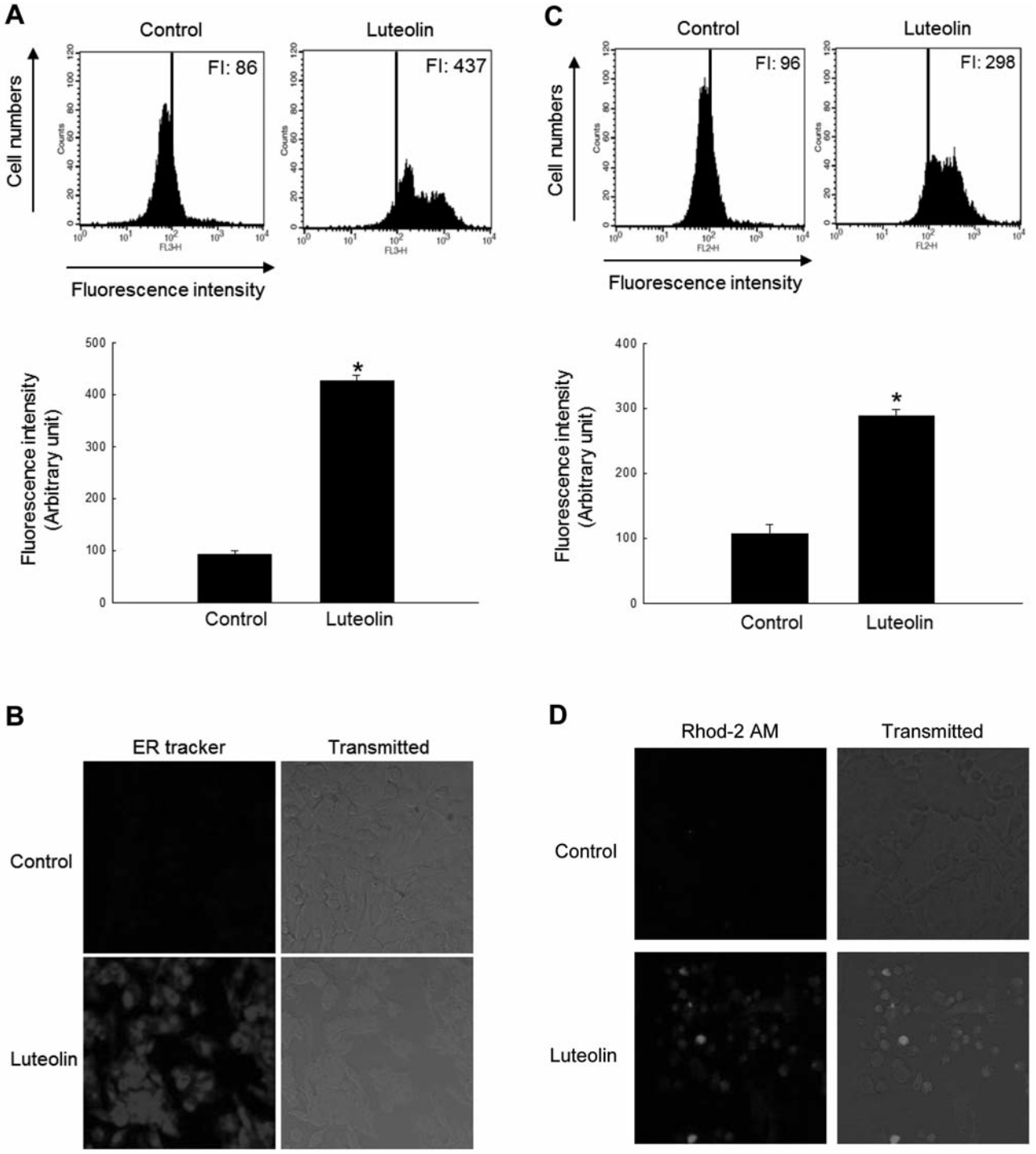

Figure 2. *Luteolin increases ER staining and mitochondrial Ca^{2+} overloading in A2058 cells. Cells were treated with luteolin for 48 h and then stained with Blue-White DPX dye. The FI in A2058 cells was measured by flow cytometry (A) and confocal microscopy (B). Representative images show the increase in the FI of the blue ER tracker in luteolin-treated cells relative to control cells. Cells were treated with luteolin for 48 h, harvested, and treated with the fluorescent probe Rhod-2 AM. Mitochondrial Ca^{2+} levels were measured via flow cytometry (C) and confocal microscopy (D). Representative images show the increase in the FI of red Rhod-2 generated by mitochondrial Ca^{2+} overloading in luteolin-treated cells relative to control cells. *Significantly different from control ($p<0.05$).*

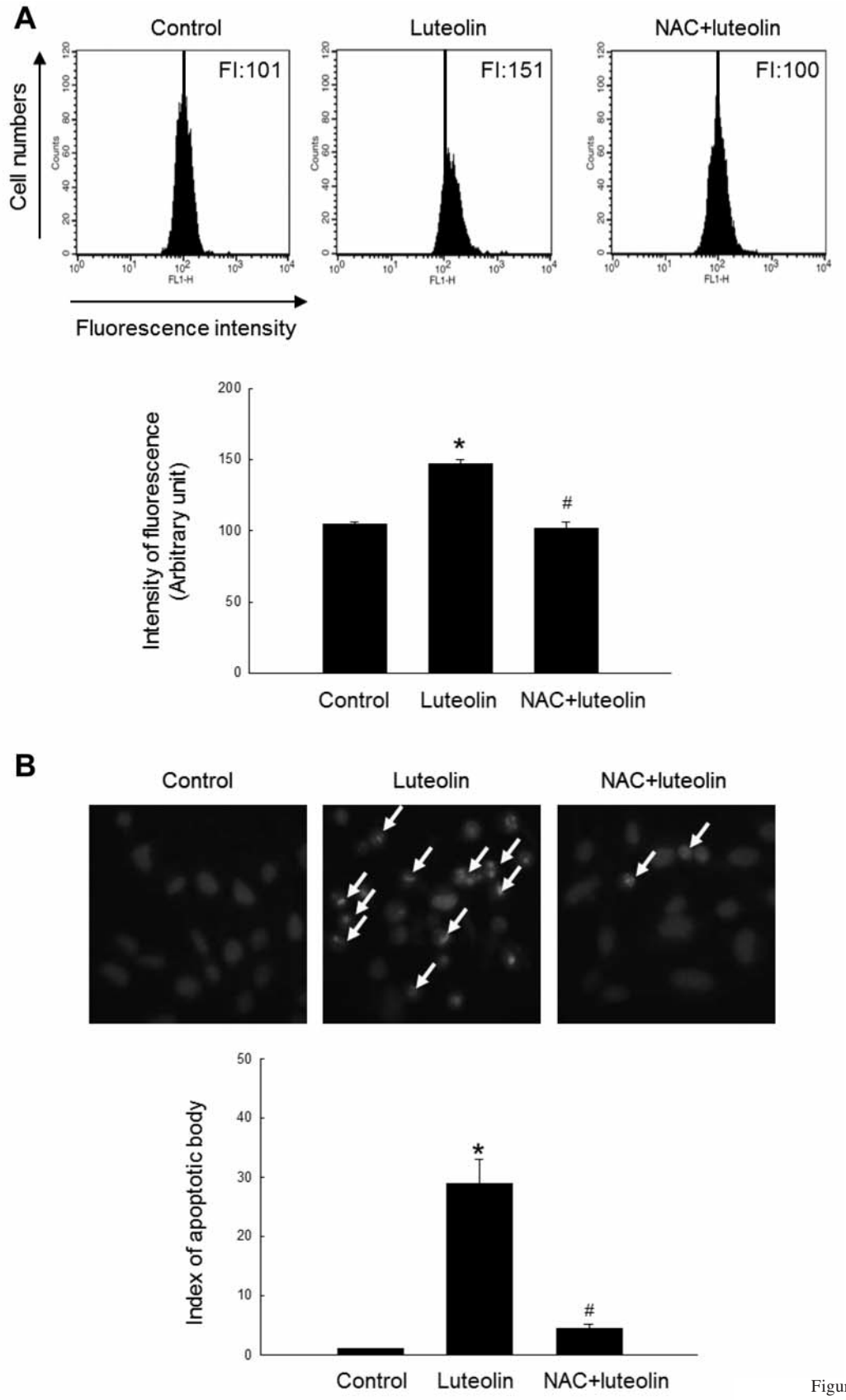

Figure 3. *continued*

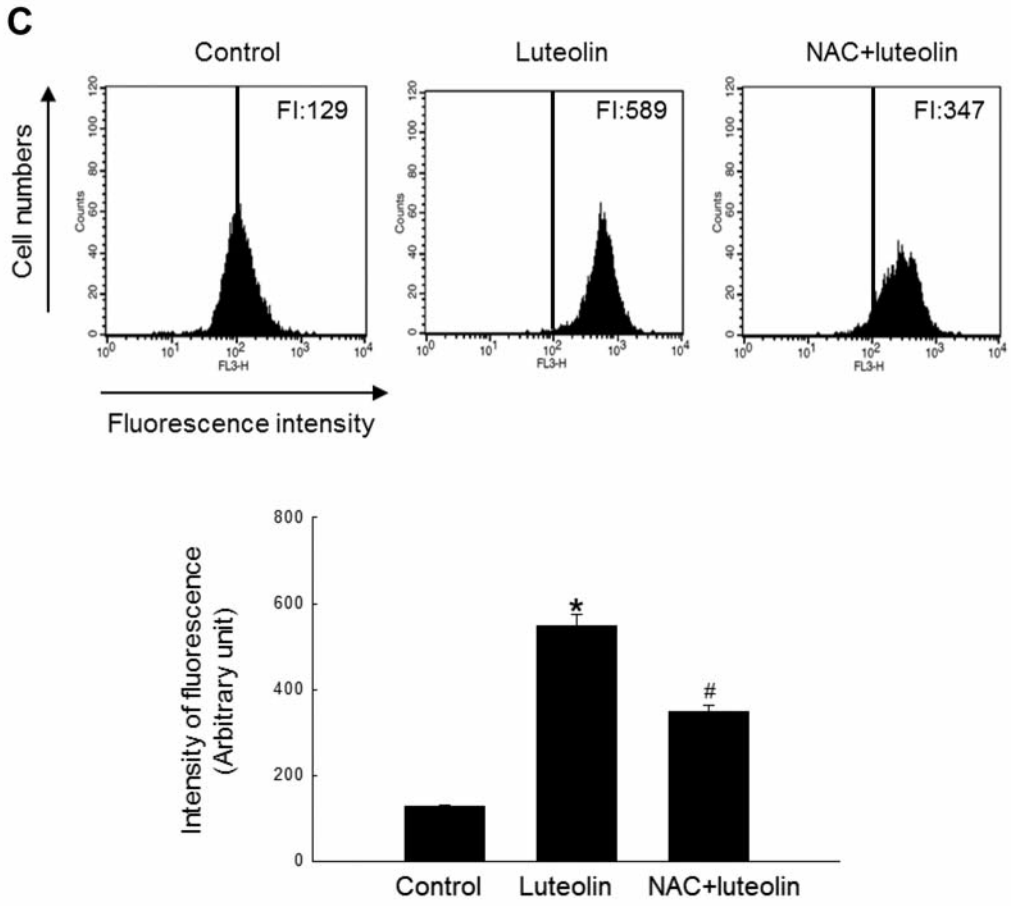

Figure 3. *Luteolin induces apoptosis and ER stress via ROS in A2058 cells. After pre-treatment with 2 mM NAC for 1 h, luteolin was added to cells and incubated for 48 h. (A) Levels of intracellular ROS were assessed in luteolin-treated cells by flow cytometry after DCF-DA staining. (B) Apoptotic body formation (arrows) was observed in luteolin-treated cells by fluorescence microscopy after Hoechst 33342 staining and quantified. (C) The ER was stained with Blue-White DPX dye and the FI was measured using flow cytometry. *Significantly different from control ($p<0.05$), and $^{\#}$significantly different from luteolin-treated cells ($p<0.05$).*

Acknowledgements

This work was supported by a research grant from Jeju National University Hospital development fund in 2015.

References

1 Staudt M, Lasithiotakis K, Leiter U, Meier F, Eigentler T, Bamberg M, Tatagiba M, Brossart P and Garbe C: Determinants of survival in patients with brain metastases from cutaneous melanoma. Br J Cancer *102*: 1213-1218, 2010.

2 Kim HJ, Lee HJ, Park MK, Gang KJ, Byun HJ, Park JH, Kim MK, Kim SY and Lee CH: Involvement of transglutaminase-2 in α-MSH-induced melanogenesis in SK-MEL-2 human melanoma cells. Biomol Ther *22*: 207-212, 2014.

3 Stutzmann GE and Mattson MP: Endoplasmic reticulum Ca^{2+} handling in excitable cells in health and disease. Pharmacol Rev *63*: 700-727, 2011.

4 Wang S and Kaufman RJ: The impact of the unfolded protein response on human disease. J Cell Biol *197*: 857-867, 2012.

5 He Y, Sun S, Sha H, Liu Z, Yang L, Xue Z, Chen H and Qi L: Emerging roles for XBP1, a sUPeR transcription factor. Gene Expr *15*: 13-25, 2010.

6 Walter P and Ron D: The unfolded protein response: from stress pathway to homeostatic regulation. Science *334*: 1081-1086, 2011.

7 Anding AL, Chapman JS, Barnett DW, Curley RW Jr and Clagett-Dame M: The unhydrolyzable fenretinide analogue 4-hydroxybenzylretinone induces the proapoptotic genes GADD153 (CHOP) and Bcl-2-binding component 3 (PUMA) and apoptosis that is caspase- dependent and independent of the retinoic acid receptor. Cancer Res *67*: 6270-6277, 2007.

8 Scaiewicz V, Nahmias A, Chung RT, Mueller T, Tirosh B and Shibolet O: CCAAT/enhancer-binding protein homologuous (CHOP) protein promotes carcinogenesis in the DEN-induced hepatocellular carcinoma model. PLoS One *8*: e81065, 2013.

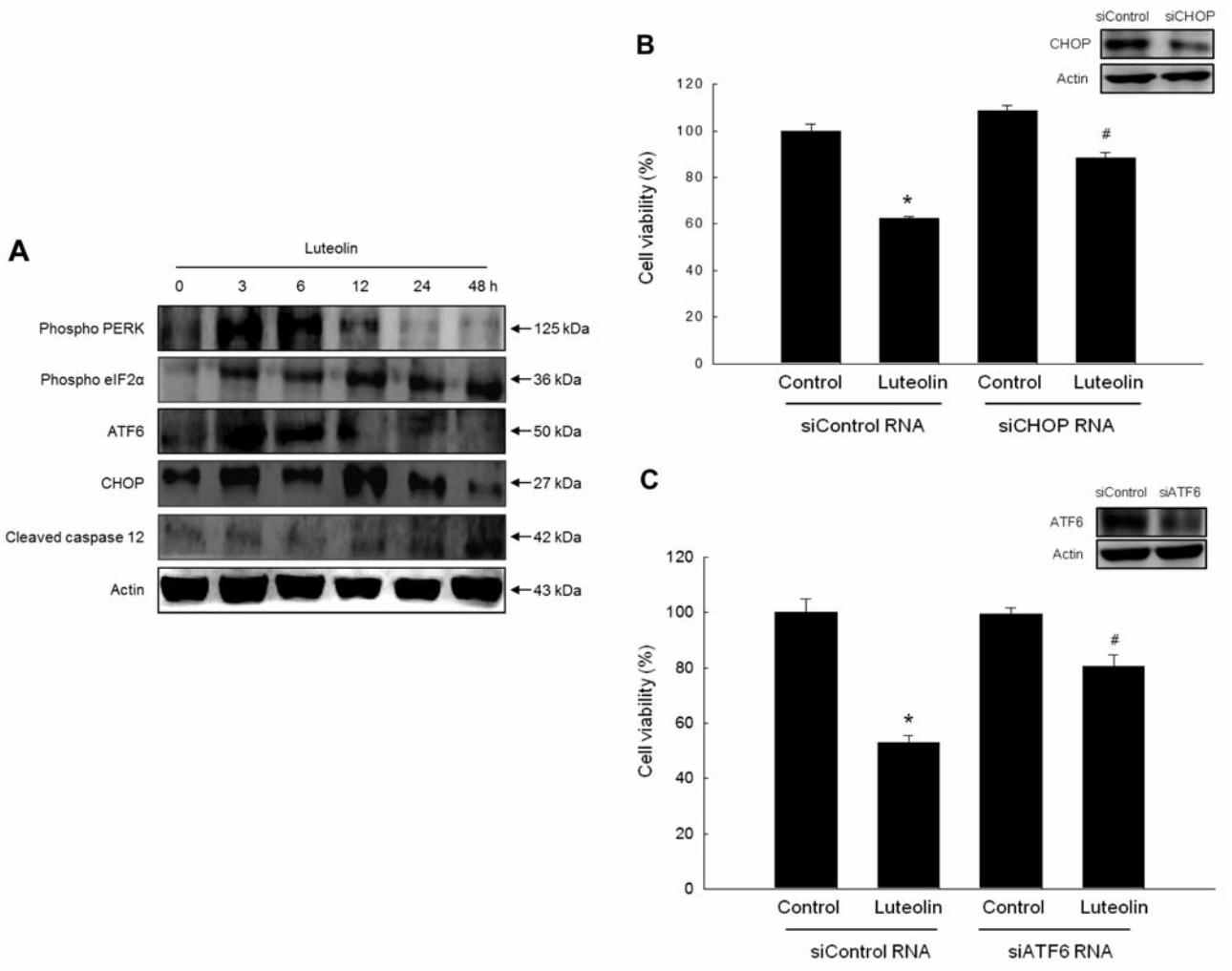

Figure 4. *Luteolin induces the expression of ER stress-related proteins in A2058 cells. (A) Cell lysates were subjected to electrophoresis, and phospho PERK, phospho eIF2α, ATF6, CHOP, and cleaved caspase 12 proteins were detected by western blotting using the appropriate specific primary antibodies. Actin was employed as a loading control. Cells were transfected with (B) siControl RNA, siCHOP RNA, or (C) siATF6 RNA for 24 h, and then treated with luteolin. After 48 h, cell viability was measured by the MTT assay. *Significantly different from control ($p<0.05$). *Significantly different from siControl-transfected cells ($p<0.05$), and #significantly different from siControl-transfected cells with luteolin treatment ($p<0.05$).*

9 Gaudette BT, Iwakoshi NN and Boise LH: Bcl-xL protein protects from C/EBP homologous protein (CHOP)-dependent apoptosis during plasma cell differentiation. J Biol Chem *289*: 23629-23640, 2014.

10 Puthalakath H, O'Reilly LA, Gunn P, Lee L, Kelly PN, Huntington ND, Hughes PD, Michalak EM, McKimm-Breschkin J, Motoyama N, Gotoh T, Akira S, Bouillet P and Strasser A: ER stress triggers apoptosis by activating BH3-only protein Bim. Cell *129*: 1337-1349, 2007.

11 Ryder CB, McColl K and Distelhorst CW: Acidosis blocks CCAAT/enhancer-binding protein homologous protein (CHOP)- and c-Jun-mediated induction of p53-upregulated mediator of apoptosis (PUMA) during amino acid starvation. Biochem Biophys Res Commun *430*: 1283-1288, 2013.

12 Bhandary B, Marahatta A, Kim HR and Chae HJ: An involvement of oxidative stress in endoplasmic retimulum stress and its associated diseases. Int J Mol Sci *14*: 434-456, 2012.

13 Sabharwal SS and Schuacker PT: Mitochondrial ROS in cancer: initiators, amplifiers or an Achilles' heel? Nat Rev Cancer *14*: 709-721, 2014.

14 Wang X, Wang B, Fan Z, Shi X, Ke ZJ and Luo J: Thiamine deficiency induces endoplasmic reticulum stress in neurons. Neuroscience *144*: 1045-1056, 2007.

15 Zhang T, Wu W, Li D, Xu T, Zhu H, Pan D, Zhu S and Liu Y: Anti-oxidant and antiapoptotic effects of luteolin on mice peritoneal macrophages stimulated by angiotensin II. Int Immunopharmacol *20*: 346-351, 2014.

16 Harris GK, Qian Y, Leonard SS, Sbarra DC and Shi X: Luteolin and chrysin differentially inhibit cyclooxygenase-2 expression and scavenge reactive oxygen species but similarly inhibit prostaglandin-E2 formation in RAW 264.7 cells. J Nutr *136*: 1517-1521, 2006.
17 Tang X, Wang H, Fan L, Wu X, Xin A, Ren H and Wang XJ: Luteolin inhibits Nrf2 leading to negative regulation of the Nrf2/ARE pathway and sensitization of human lung carcinoma A549 cells to therapeutic drugs. Free Radic Biol Med *50*: 1599-1609, 2011.
18 Choi AY, Choi JH, Yoon H, Hwang KY, Noh MH, Choe W, Yoon KS, Ha J, Yeo EJ and Kang I: Luteolin induces apoptosis through endoplasmic reticulum stress and mitochondrial dysfunction in Neuro-2a mouse neuroblastoma cells. Eur J Pharmacol *668*: 115-126, 2011.
19 Park SH, Ham S, Kwon TH, Kim MS, Lee DH, Kang JW, Oh SR and Yoon DY: Luteolin induces cell cycle arrest and apoptosis through extrinsic and intrinsic signaling pathways in MCF-7 breast cancer cells. J Environ Pathol Toxicol Oncol *33*: 219-231, 2014.
20 Pandurangan AK and Ganapasam S. Cytotoxic effect of luteolin on human colorectal cancer cell line (HCT-15): crucial involvement of reactive oxygen species. Middle East J Cancer *4*: 177-182, 2013.
21 Hwang YJ, Lee EJ, Kim HR and Hwang KA: Molecular mechanisms of luteolin-7-O-glucoside-induced growth inhibition on human liver cancer cells: G_2/M cell cycle arrest and caspase-independent apoptotic signaling pathways. BMB reports *46*: 611-616, 2013.
22 Ma L, Peng H, Li K, Zhao R, Li L, Yu Y, Wang X and Han Z: Luteolin exerts an anticancer effect on NCI-H460 human non-small cell lung cancer cells through the induction of Sirt1-mediated apoptosis. Mol Med Rep *12*: 4196-4202, 2015.
23 Ju SM, Youn GS, Cho YS, Choi SY and Park J: Celastrol ameliorates cytokine toxicity and pro-inflammatory immune responses by suppressing NF-κB activation in RINm5F beta cells. BMB Rep *48*: 172-177, 2015.
24 Eruslanov E and Kusmartsev S: Identification of ROS using oxidized DCFDA and flow-cytometry. Methods Mol Biol *594*: 57-72, 2010.
25 Hammadi M, Oulidi A, Gackiere F, Katsogiannou M, Slomianny C, Roudbaraki M, Dewailly E, Delcourt P, Lepage G, Lotteau S, Ducreux S, Prevarskaya N and Van Coppenolle F: Modulation of ER stress and apoptosis by endoplasmic reticulum calcium leak *via* translocon during unfolded protein response: involvement of GRP78. *27*: 1600-1609, 2013.
26 Park HK, Lee JE, Lim J and Kang BH: Mitochondrial Hsp90s suppress calcium-mediated stress signals propagating from mitochondria to the ER in cancer cells. Mol Cancer *13*: 148, 2014.
27 Pinton P, Giorgi C, Siviero R, Zecchini E and Rizzuto R: Calcium and apoptosis: ER-mitochondria Ca^{2+} transfer in the control of apoptosis. Oncogene *27*: 6407-6418, 2008.
28 Kim I, Xu W and Reed JC. Cell death and endoplasmic reticulum stress: disease relevance and therapeutic opportunities. Nat Rev Drug Discov *7*: 1013-1030, 2008.
29 Verfaillie T, Garg AD and Agostinis P: Targeting ER stress induced apoptosis and inflammation in cancer. Cancer Lett *332*: 249-264, 2013.
30 Hotokezaka Y, van Leyen K, Lo EH Beatrix B, Katayama I, Jin G and Nakamura T: alphaNAC depletion as an initiator of ER stress-induced apoptosis in hypoxia. Cell Death Differ *16*: 1505-1514, 2009.
31 Brisac C, Téoulé F, Autret A, Pelletier I, Colbère-Garapin F, Brenner C, Lemaire C and Blondel B: Calcium flux between the endoplasmic reticulum and mitochondrion contributes to poliovirus-induced apoptosis. J Virol *84*: 12226-12235, 2010.
32 Mikoshiba K: Inositol 1,4,5-trisphosphate IP(3) receptors and their role in neuronal cell function. J Neurochem *97*: 1627-1633, 2006.
33 Wali VB, Bachawal SV and Sylvester PW: Endoplasmic reticulum stress mediates gamma-tocotrienol-induced apoptosis in mammary tumor cells. Apoptosis *14*: 1366-1377, 2009.
34 Seo K, Ki SH and Shin SM: Methylglyoxal induces mitochondrial dysfunction and cell death in liver. Toxicol Res *30*: 193-198, 2014.

Received February 3, 2016
Revised April 7, 2016
Accepted April 8, 2016